Biochimica et Biophysica Acta 1821 (2012) 706–718

Contents lists available at SciVerse ScienceDirect

Biochimica et Biophysica Acta

journal homepage: www.elsevier.com/locate/bbalip

Uptake and protein targeting of fluorescent oxidized phospholipids in cultured RAW 264.7 macrophages

U. Stemmer [a], C. Ramprecht [a], E. Zenzmaier [a], B. Stojčić [a], G. Rechberger [b], M. Kollroser [c], A. Hermetter [a,*]

[a] Institute of Biochemistry, Graz University of Technology, Petersgasse 12/II, A-8010 Graz, Austria
[b] Institute of Molecular Bioscience, University of Graz, Humboldtstraße 50/II, A-8010 Graz, Austria
[c] Institute of Forensic Medicine, Medical University of Graz, Universitätsplatz 4/II, A-8010 Graz, Austria

ARTICLE INFO

Article history:
Received 13 July 2011
Received in revised form 12 January 2012
Accepted 18 January 2012
Available online 8 February 2012

Keywords:
Aldehydophospholipid
Schiff base
Atherosclerosis
Phospholipid exchange
Oxidized LDL
Functional proteomic analysis

ABSTRACT

The truncated phospholipids 1-palmitoyl-2-(5-oxovaleroyl)-*sn*-glycero-3-phosphocholine (POVPC) and 1-palmitoyl-2-glutaroyl-*sn*-glycero-3-phosphocholine (PGPC) are oxidation products of 1-palmitoyl-2-arachidonoyl phosphatidylcholine. Depending on concentration and the extent of modification, these compounds induce growth and death, differentiation and inflammation of vascular cells thus playing a role in the development of atherosclerosis. Here we describe the import of fluorescent POVPC and PGPC analogs into cultured RAW 264.7 macrophages and the identification of their primary protein targets. We found that the fluorescent oxidized phospholipids were rapidly taken up by the cells. The cellular target sites depended on the chemical reactivity of these compounds but not on the donor (aqueous lipid suspension, albumin or LDL). The great differences in cellular uptake of PGPC and POVPC are a direct consequence of the subtle structural differences between both molecules. The former compound (carboxyl lipid) can only physically interact with the molecules in its immediate vicinity. In contrast, the aldehydo-lipid covalently reacts with free amino groups of proteins by forming covalent Schiff bases, and thus becomes trapped in the cell surface. Despite covalent binding, POVPC is exchangeable between (lipo) proteins and cells, since imines are subject to proton-catalyzed base exchange. Protein targeting by POVPC is a selective process since only a limited subfraction of the total proteome was labeled by the fluorescent aldehydo-phospholipid. Chemically stabilized lipid–protein conjugates were identified by MS/MS. The respective proteins are involved in apoptosis, stress response, lipid metabolism and transport. The identified target proteins may be considered primary signaling platforms of the oxidized phospholipid.

1. Introduction

vascular wall is a hallmark of atherosclerosis [1]. This process is mediated by the scavenger receptor and is not regulated. As a consequence, massive amounts of lipid accumulate in these cells. The macrophages change their phenotype and become foam cells, leading

ial space, an early
enger receptor is
e particle surface
due to covalent modification of apoB lysines by lipid aldehydes that are oxidation products of polyunsaturated (phospho)lipids [2]. To some extent, oxidized fatty acids and phospholipids containing free carboxyl groups also contribute to this characteristic signature of oxLDL. The harmful effects of oxLDL are not only associated with lipid accumulation in macrophages and other vascular (smooth muscle) cells (*lipotoxicity*). They are also mediated by the intrinsic toxicity of a great variety of lipid oxidation products that are generated in LDL under the conditions of oxidative stress (*lipid toxicity*) [3,4]. These compounds comprise oxidized sterols, oxidized fatty acid derivatives and oxidized glycerophospholipids. They have been found in plasma LDL and in lipid deposits as well as lipoproteins isolated from atherosclerotic plaques [5]. The main phospholipid species in the LDL surface contain linoleic and to a lesser extent arachidonic acid in position *sn*-2 of glycerol [6]. Their oxidation products may contain a modified long-chain carboxylic acid in this position or a truncated acyl residue with a polar functional group at its ω-end. Typical

Abbreviations: aSMase, acid sphingomyelinase; BSA, bovine serum albumin; BY, BODIPY™; DMEM, Dulbecco's modified Eagle's medium; HAEC, human aortic endothelial cells; IL, interleukin; LDL, low density lipoprotein; MAPK, mitogen-activated protein kinase; mmLDL, minimally modified LDL; oxLDL, oxidized LDL; oxPL, oxidized phospholipids; PAF, platelet activating factor; PAPC, 1-palmitoyl-2-arachidonoyl-*sn*-glycero-3-phosphocholine; Paze-PC, 1-palmitoyl-2-azelaoyl-sn-glycero-3-phosphocholine; PC, phosphatidylcholine; PE, phosphatidylethanolamine; PGPC, 1-palmitoyl-2-glutaroyl-*sn*-glycero-3-phosphocholine; POPE, 1-palmitoyl-2-oleoyl-*sn*-glycero-3-phosphoethanolamine; POVPC, 1-palmitoyl-2-(5-oxovaleroyl)-*sn*-glycero-3-phosphocholine; Poxno-PC, 1-palmitoyl-2-(9-oxo-nonanoyl)-*sn*-glycero-3-phosphocholine; PS, phosphatidylserine; ROS, reactive oxygen species; TCA, trichloroacetic acid; TLC, thin layer chromatography; TLR, toll-like receptor; VDAC, voltage dependent anion channel

* Corresponding author. Tel.: +43 316 873 6457; fax: +43 316 873 6952.
E-mail address: albin.hermetter@tugraz.at (A. Hermetter).

1388-1981 © 2012 Elsevier B.V. Open access under CC BY-NC-ND license.
doi:10.1016/j.bbalip.2012.01.014

derivatives of truncated phospholipids are the chemically reactive aldehydophospholipids POVPC and Poxno-PC (from arachidonoyl- and linoleoyl phospholipids, respectively) and the carboxy-phospholipids PGPC and Paze-PC (also from arachidonoyl- and linoleoyl phospholipids, respectively). We found that sustained exposure towards μM concentrations of both phospholipid classes induces apoptosis in vascular cells including vascular smooth muscle cells [7] and macrophages (Stemmer et al., unpublished data). Programmed cell death is mediated by ceramide which is formed as a consequence of the rapid activation of acid sphingomyelinase, very likely on the protein level [8]. The same effects were observed, when the cells were treated with minimally modified LDL under the same conditions. This particle can be obtained by mild oxidation of LDL *in vitro* and is perhaps a reliable model for the oxidized LDL formed *in vivo*. It is characterized by a high content of lipid oxidation products and a low degree of protein modification. Therefore, it is still recognized by the LDL receptor. As a consequence its toxicity must be largely due to the effects of its oxidized (phospho)lipid components.

Truncated phospholipids contain only a single hydrophobic long-chain fatty acid in position *sn*-1 attaching the amphiphile to the hydrophobic domain of the bilayer. From molecular dynamics studies, it can be inferred that the truncated *sn*-2 fatty acid folds back to the aqueous phase (carboxylic-phospholipids) or the lipid–water interface (aldehydo-phospholipids) [9]. Therefore, these compounds show similar (supra)molecular features compared with other biologically active phospholipids, namely lysolecithin and platelet activating factor (PAF) [5].

Uptake and activity of oxidized phospholipids in cells have extensively been discussed in the context of receptor-mediated processes. Typical candidates are CD36 recognizing negatively charged motifs, *e.g.* due to carboxy-phospholipids, or the PAF receptor with affinities for choline phospholipids containing short *sn*-2 acyl chains [10]. In addition to the capacity of the oxidized phospholipids to interact with receptors, their highly amphipathic character contributes to their cellular activities. Unlike entirely water-soluble receptor ligands, they efficiently partition into phospholipid bilayers where they can affect the functions of membrane-bound (signaling) proteins either by direct interactions or in an indirect way by modulating lipid dynamics and organization. Thus, it is more likely that oxidized phospholipids encounter many primary targets representing primary signaling platforms either in the plasma membrane or after rapid internalization inside the cells.

In this study we characterized the import of fluorescent analogs of the oxidized phospholipids POVPC and PGPC into cultured RAW 264.7 macrophages and identified their potential primary protein targets. The fluorescently labeled lipid analogs [11] were used as molecular tools to visualize these processes and detect the lipid binding polypeptides. We found that the fluorescent oxidized phospholipids were rapidly taken up by the cells. Lipid import and localization depended on the chemical reactivity of these compounds (aldehydo *versus* carboxylate derivative). The lipid donor (aqueous lipid suspension, albumin, LDL) hardly showed any effect, pointing to the transfer of single molecules between the donor and acceptor surfaces. Targeting of cellular proteins is a selective process since only a subfraction of the total proteome was labeled. The respective lipid-associated proteins may be considered primary signaling platforms of oxPL.

2. Materials and methods

2.1. Materials

Oxidized phospholipids (PGPC and POVPC) and their fluorescent analogs (BY-PGPE and BY-POVPE) were synthesized in our laboratory as previously described [11]. Chemicals for gel electrophoresis were from BioRad Laboratories (Hercules, CA), unless otherwise noted. Organic solvents and all other chemicals were purchased from Carl Roth (Karlsruhe, Germany) or Sigma-Aldrich (Steinheim, Germany). Tissue culture materials were obtained from Sarstedt (Nümbrecht, Germany) or Greiner (Kremsmünster, Austria). Dulbecco's modified Eagle's medium and heat-inactivated fetal bovine serum were from Invitrogen (Leek, Netherlands), and PBS and other cell culture supplements were obtained from PAA (Linz, Austria), unless otherwise indicated.

2.2. LDL isolation and modification

Human LDL was isolated from pooled fresh plasma (a kind gift of Dr. Gholam Ali Khoschsorur, University Hospital, Graz) by density ultracentrifugation in OptiSeal tubes using a Beckman NVT65 Rotor [12]. The LDL fraction was collected and transferred into sterile septum vials (TechneVials, Mallinckrodt, Germany) and stored at 4 °C until use within 2 weeks of isolation. Lipoprotein concentration is expressed in terms of protein content, which was measured in a plate assay according to the method of Bradford [13]. LDL was desalted using PD 10 columns (GE Healthcare, Munich, Germany) prior to modification or labeling and diluted to 50 or 100 μg protein/ml, if not stated otherwise. Minimally modified LDL (mmLDL) was prepared as previously described [14]. LDL was incubated with 10 μM $FeSO_4$ in sterile H_2O at room temperature for 24 h. mmLDL was desalted using PD 10 column (GE Healthcare, Munich, Germany) prior to use.

2.3. Delivery systems for fluorescently labeled oxPLs

Lipid dispersions containing 5 or 10 μM lipid in PBS buffer were prepared using the ethanol injection method [15]. The final ethanol concentrations did not exceed 1% (v/v). Albumin-oxPL complexes (protein/lipid = 1/1 mol/mol) were prepared, using the same technique. For this purpose, ethanolic solutions of oxPL were injected into solutions of BSA in PBS under stirring at 37 °C. Concentration of fluorescent oxPL was 5 μM. (mm)LDL-oxPL complexes (apoB100/oxPL = 20/1 mol/mol) were prepared by injection of ethanolic lipid solutions into LDL suspensions (50 μg protein/ml) at 37 °C followed by incubation at room temperature for 30 min. Total oxPL concentrations were 5 μM. Labeled LDL preparations were analyzed using native agarose gel electrophoresis (0.5% agarose gel, 80 V). Fluorescently labeled LDL was visualized in-gel using a Herolab imager (excitation wavelength: 365 nm) driven by EasyWin software. Total protein was stained with Coomassie blue (0.02%, w/v). Fluorescently labeled proteins in albumin and LDL preparations were precipitated according to Wessel and Flügge [16], separated by SDS-PAGE (4.5% stacking gel, 10% resolving gel) according to Fling and Gregerson [17] and visualized using a BioRad laser scanner (Ex 488 nm, Em 530/30 BP). Finally, total protein was stained using SYPRO Ruby™ (Invitrogen) according to manufacturer's instruction. SDS gels were scanned for fluorescence at 605 nm upon excitation with a 488 nm laser. Incubations of the cells with pure lipid dispersions or lipid-carrier complexes were performed in PBS or media without phenol red at varying concentrations of FBS (0–10% v/v).

2.4. Cell culture

The macrophage cell line RAW 264.7 (ATCC No. TIB-71, American Type Culture Collection, Rockville, MD, USA) was a kind gift from Dagmar Kratky, Medical University of Graz, Austria. Cells were routinely grown in DMEM (4.5 g/l glucose, 25 mM HEPES, 4 mM L-glutamine, without sodium pyruvate) supplemented with 10% heat-inactivated FBS and 100 U/ml penicillin/streptomycin at 37 °C in humidified CO_2 (5%) atmosphere.

2.5. Fluorescence microscopy

Monolayer cultures of RAW 264.7 cells were grown to 60–80% confluency in Chamber slides (Nunc, Nalgene, Rochester USA). Cells were incubated with aqueous dispersions of oxPLs or oxPL-carrier complexes (total concentrations of fluorescent oxPL were 5 or

10 μM) for 5 or 30 min, if not otherwise indicated. After incubation, cells were carefully rinsed with PBS and observed with an Axiovert 35 inverted fluorescence microscope equipped with a mercury-arc lamp and a CCD camera, driven by AxioVision software package (Carl Zeiss, Germany). BY-fluorescence (Ex 505 nm, Em 510 nm) was detected using the following filter set: excitation filter BP 450–490 nm, beam splitter 510 nm and barrier filter LP 520 nm. Unlabeled cells were used as a reference to examine autofluorescence.

For fluorescence colocalization experiments monolayer cultures of RAW 264.7 cells were grown to 60–80% confluency in Chamber slides (Nunc, Nalgene, Rochester USA). Cells were incubated with 10 μM oxPLs in PBS for 30 min. The labeled cells were rinsed twice with PBS prior to incubation with 5 μg/ml Cellmask Deep Red plasma membrane stain diluted in PBS (Invitrogen) for 10 min. Finally, cells were washed three times with PBS and BY fluorescence was observed with an Axiovert 35 inverted fluorescence microscope as described above. Cellmask fluorescence (Ex 649, Em 666) was detected using the following filter set: excitation filter BP 575–625, beam splitter 645 and emission filter 660–710.

2.6. BY-POVPE exchange between cells, LDL and albumin

Solutions of BY-POVPE/LDL complexes in PBS (apoB/oxPL = 20/1 mol/mol, total oxPL concentration 5 μM) were desalted using PD 10 columns prior to incubation with 5 μM BSA solutions in PBS (molar ratios of apoB100/albumin were 1:1, 1:5 and 1:10). The mixtures were incubated for 30 min at room temperature. Proteins were precipitated according to the method of Wessel and Flügge [16] and separated by SDS-PAGE [17] (4.5% stacking gel, 10% resolving gel). Fluorescently labeled proteins were detected using a BioRad laser scanner (Ex 488 nm, Em 530/30). Backtransfer of BY-POVPE from cells to albumin was measured as follows: RAW 264.7 cells were grown to 60–80% confluency in 100 mm Petri dishes and treated with 6 ml of 5 μM fluorescent lipid in PBS as described above for 15 min. After washing the cells three times with PBS, 5 μM BSA in PBS was added followed by incubation at 37 °C (5% CO_2) for 15 min. The supernatant was isolated and the fluorescent proteins were separated by SDS-PAGE and imaged as described above.

2.7. Determination of protein targets of BY-POVPE

2.7.1. Separation of total cell proteins by 2-D electrophoresis

RAW 264.7 cells grown to 80% confluency in 175 cm^2 culture flasks were incubated with 10 ml 10 μM BY-POVPE dispersion in PBS in the dark for 30 min. Labeled cells were washed twice with cold PBS and scraped into 3 ml washing solution (PBS supplemented with 100 mg/ml $CaCl_2$, 10 mg/ml $MgCl_2$, 1 mM PMSF and 50 μM $NaCNBH_3$). The following steps were performed at 4 °C. Cells were centrifuged at 300 *g* for 3 min. The supernatant was discarded, followed by cell lysis in 150 μl of lysis buffer, containing 20 mM HEPES, 2 mM EDTA, 1% (v/v) Triton X-100 pH 7.4, 50 μM $NaCNBH_3$, 1 mM PMSF, 10 μg/ml SBTI, 10 μg/ml leupeptin, for 1 h on ice. The cell suspension was vigorously vortexed every 15 min. The lysate was centrifuged at 1000 *g* for 5 min. $NaCNBH_3$ was added to the supernatant (final concentration 100 μM). The resultant solution was incubated at 37 °C for 2 h and stored at −20 °C. Protein concentration was determined using a plate assay based on the method of Bradford [13]. For 2-D PAGE on 20 × 20 cm gels, 500 μg protein was precipitated by TCA or according to the method of Wessel and Flügge [16]. The protein pellet was solubilized in 340 μl rehydration buffer, containing 7 M urea, 2 M thiourea, 4% Chaps, 0.002% bromphenol blue and 2% Pharmalyte™ 3–10, at 37 °C for 30 min. Sample solutions were applied to 18 cm immobilized pH gradient strips pH 3–10 (GE Healthcare, Munich, Germany). Strips were incubated over night at room temperature in the dark. Isoelectric focusing and subsequent SDS-PAGE were performed as previously described [18]. Electrophoretic separation of proteins was performed using a PROTEAN II Multi cell apparatus. After electrophoresis, gels were fixed in aqueous solution containing 10 vol.% EtOH and 7 vol.% AcOH, for at least 2 h. BY-fluorescence was detected using a BioRad laser scanner (Ex 488 nm, Em 530/30 BP). Total proteins were stained with SYPRO Ruby™ (Ex 488 nm, Em 605 nm).

2.7.2. Separation of membrane proteins by 1-D gel electrophoresis

RAW 264.7 cells grown to 80% confluency in 175 cm^2 culture flasks were incubated with 10 ml aqueous solutions of BY-POVPE in the dark for 30 min. Labeled cells were washed twice with cold PBS and scraped into 10 ml PBS and isolated by centrifugation at 300 *g* for 5 min. The cell pellet was resuspended in 1 ml homogenization buffer (0.218 M sucrose, 10 mM Tris/HCl, 1 mM EDTA, pH 7.4) and separated by centrifugation at 450 *g* for 5 min. The pellet was resuspended in homogenization buffer (1.5 fold pellet volume) supplemented with aprotinin, pepstatin, leupeptin, (10 μg/ml each), 0.8 mM PMSF, 30 μg/ml cycloheximin and 50 μM $NaCNBH_3$. The following steps were performed at 4 °C. Labeled cells were homogenized using a glass–glass homogenizer. The extent of homogenization was monitored by light microscopy. Homogenized cells were centrifuged at 600 *g* for 10 min. The post nuclear supernatant (PNS) was centrifuged again at 600 *g* for 5 min. The PNS was diluted with homogenization buffer containing the protease inhibitors indicated above (final volume 800 μl) and the sample was transferred into Beckmann centrifuge tubes (11 × 34) for ultracentrifugation (142,000 × *g*) at 4 °C for 1 h. The obtained supernatant represents the cytosolic fraction. The membrane pellet was washed in 800 μl homogenization buffer containing the protease inhibitors indicated above and centrifuged at 117,000 *g* at 4 °C for 1 h. The membrane pellet was resuspended in 200 μl homogenization buffer. $NaCNBH_3$ (final concentration 100 μM) was added to the PNS, the cytosolic fraction and the membrane fraction followed by incubation at 37 °C for 2 h. Samples were stored at −20 °C. For 1-D SDS-PAGE, protein concentration was determined using a plate assay based on the method of Bradford [13]. 100 μg protein of each sample was precipitated according to Wessel and Flügge [16] and dissolved in 50 μl loading buffer [17]. The samples were applied onto a 20 × 20 cm SDS gel prepared and separated according to the PROTEAN II xi cell protocol provided by BioRad. Gels were fixed over night in aqueous solutions containing 10 vol.% EtOH and 7 vol.% AcOH. BY-fluorescence was imaged using a BioRad laser scanner (Ex 488 nm, Em 530/30 BP). Total proteins were stained with SYPRO Ruby™ as indicated above.

Inhibitory effect of POVPC on protein labeling with BY-POVPE:

a) Albumin labeling. An ethanolic solution of a mixture of POVPC/BY-POVPE was injected into PBS containing 5 μM bovine serum albumin at room temperature under stirring for 30 min. Final lipid concentrations were 0–100 μM POVPC and 5 μM BY-POVPE. $NaCNBH_3$ (final concentration 10 mM) was added and imines were reduced for 30 min. Protein separation and fluorescence detection on acrylamide gels were performed as described above.
b) Labeling of cell proteins. Cultured RAW macrophages (9×10^6 cells, 30 cm^2) were incubated in DMEM without Phenol red, containing 0.1% FCS and a mixture of POVPC (50 μM)/BY-POVPE (5 μM). Labeled cells were washed with PBS containing 10 mM $NaCNBH_3$. Cells were scraped off and isolated by centrifugation (300 *g*, 4 °C, 5 min). The cell pellet was resuspended in 500 μl PBS containing 10 mM $NaCNBH_3$ and disintegrated by pulsed ultrasonication (15 pulses for 1 s) at 4 °C. After centrifugation (1000 *g*, 4 °C, 10 min), the supernatant was isolated. After addition of $NaCNBH_3$ (final concentration 10 mM), the solution was stirred at room temperature for 30 min. Protein separation and fluorescence detection on acryl amide gels were performed as described above.

2.7.3. Tryptic digest and MS/MS analysis

Fluorescent BY-POVPE-protein complexes were excised from acryl amid gels and tryptically digested according to the method of Shevchenko et al. [19]. Peptide extracts were dissolved in 0.1% formic acid and separated by nano-HPLC-system (ULTIMATE™ 3000 nanoLC system, Dionex, Amsterdam, The Netherlands) as described [20], but using the following gradient: solvent A: water, 0.3% formic acid; solvent B: acetonitrile/water 80/20 (v/v), 0.3% formic acid; 0–5 min: 4% B, after 40 min 55% B, then for 5 min 90% B, and 47 min reequilibration at 4% B. The peptides were ionized in a Finnigan nano-ESI source equipped with Nanospray tips (PicoTip™ Emitter; New Objective, Woburn, MA) and analyzed in a Thermo-Finnigan LTQ linear iontrap mass-spectrometer (Thermo, San Jose, CA). The MS/MS data were analyzed by searching the National Center for Biotechnology Information nonredundant public database with SpektrumMill Rev.03.03.084 (Agilent, Darmstadt, Germany) software. Acceptance parameters were two or more identified distinct peptides according to Carr et al. [21]. Identified protein sequences were subjected to BLAST and other public databases (NCBI, SwissProt, Expasy, Brenda) to search for protein target candidates.

3. Results

We report on the cellular uptake and the primary molecular targets of a subclass of oxidized phosphatidylcholines. The respective compounds contain a long-chain fatty acid in position *sn*-1 and a short, polar, acyl chain in position *sn*-2 of glycerol thus roughly resembling the chemical structure of platelet activating factor [5,4]. However, it has to be emphasized that the latter phospholipid exclusively contains a short but unpolar acetyl residue at this position. Specifically, we compared two compounds showing the same structural features except for the functional group at the ω-end of the *sn*-2 chain (Fig. 1). In PGPC, this is a carboxylate residue which renders the entire molecule negatively charged. POVPC contains an aldehyde function which is less polar but chemically reactive and thus can undergo Schiff base formation with the free amino groups of proteins or phospholipids [22]. In this study, we used BY-PGPE and BY-POVPE, as fluorescently labeled analogs of PGPC and POVPC respectively, carrying a polar BY-fluorophore linked to the polar lipid head groups (Fig. 1) [11]. These compounds were used for visualization of lipids in live cells and lipid–protein complexes in acryl amide or agarose gels. In a previous study, we have provided evidence that they are reliable model compounds of their unlabeled counterparts [11].

Under physiological conditions, polar lipids can be transferred to cells from different molecular and supramolecular systems such as plasma proteins (albumin) and (low) density lipoproteins. Therefore, we prepared and characterized different donors containing the fluorescent lipid analogs and investigated the transfer of the labeled lipids from these systems to cultured macrophages using fluorescence microscopy. Conversely, we studied lipid transfer between the individual donors and the back-transfer of the lipids from the cells to the donors. Donor systems for our *in vitro* studies were defined complexes of the fluorescent lipids with albumin and LDL as well as aqueous lipid dispersions as reference systems. Fig. 2 describes the characterization of BY-POVPE complexes with LDL and albumin. Agarose gel electrophoresis shows uniform bands of the fluorescent LDL (Fig. 2A). Fluorescence and protein detection demonstrate that the electrophoretic mobility of the labeled particle is higher as compared to unlabeled LDL. This effect is due to a more negative net charge which is a consequence of covalent modification of the LDL amino groups by the phospholipid aldehyde. SDS electrophoresis supports the assumption of an LDL-fluorophore complex containing covalently labeled apolipoprotein B (apo B) (Fig. 2B). No fluorescence is seen in apo B in SDS-PAGE after incubation with the carboxy lipid BY-PGPE because lipid–protein interaction is noncovalent in this system. The latter lipid can only be detected in LDL after running the labeled lipoprotein under conditions of native agarose gel electrophoresis (data not shown).

Both fluorescent oxidized phospholipids form complexes with serum albumin. This observation is in line with the affinity of this protein for other phospholipids containing only one long-chain fatty acid (*e.g.* lysophospholipids) [23]. BY-POVPE also forms a stable complex with albumin which is detectable by fluorescence imaging after SDS gel electrophoresis (Fig. 2B). In order to observe phospholipid transfer independent of receptor-mediated endocytosis, uptake of fluorescent oxPL into the cells was studied under growth conditions, where the LDL receptor was not expressed. BY-PGPE and BY-POVPE are taken up into these cells in a very different manner (Fig. 3A). BY-PGPE is quickly internalized. The amount of fluorophore residing in the plasma membrane must be negligible since only a small fraction of the fluorescent cellular lipid can be extracted by aqueous Triton X-100 (data not shown). The mechanism of lipid uptake has already been described in a previous publication. It has been shown that the fluorescent compound inserts into the plasma membrane followed by cluster formation within milliseconds [24]. Eventually, the fluorescent domains are internalized by endocytosis. BY-POVPE mainly localizes to the cell surface (colocalization with a plasma membrane-specific dye; Fig. 3B), due to Schiff base formation with membrane proteins and amino phospholipids. The lipid–protein complexes were stabilized by chemical reduction and identified as putative primary targets of the phospholipid aldehyde (see below).

In summary, lipid uptake does not depend on the donor system. The same cellular fluorescence patterns were obtained if phospholipids were released to the cells from pure lipid dispersions, lipid–albumin complexes or lipid-loaded LDL (Fig. 3C). However, the fluorescence intensity of BY-PGPE inside the cells was significantly lower if labeled LDL was the lipid donor. This lipoprotein contains PAF-acetylhydrolase which also catalyzes the degradation of short-

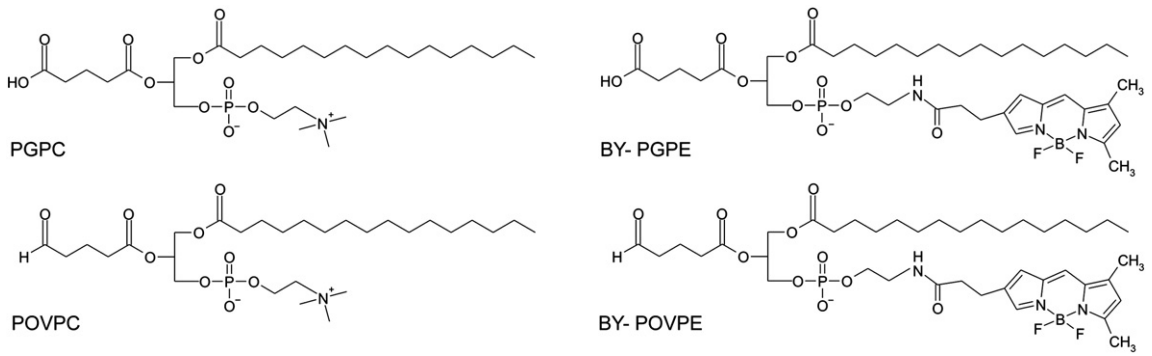

Fig. 1. Chemical structures of oxPLs and their fluorescent analogs.PGPC: 1-Palmitoyl-2-glutaroyl-*sn*-glycero-3-phosphocholine. BY-PGPE: 1-Palmitoyl-2-glutaroyl-*sn*-glycero-3-phospho-N-BODIPY™-ethanolamine. POVPC: 1-Palmitoyl-2-(5-oxovaleroyl)-*sn*-glycero-phosphocholine. BY-POVPE: 1-Palmitoyl-2-(5-oxovaleroyl)-*sn*-glycero-phospho-N-BODIPY™-ethanolamine.

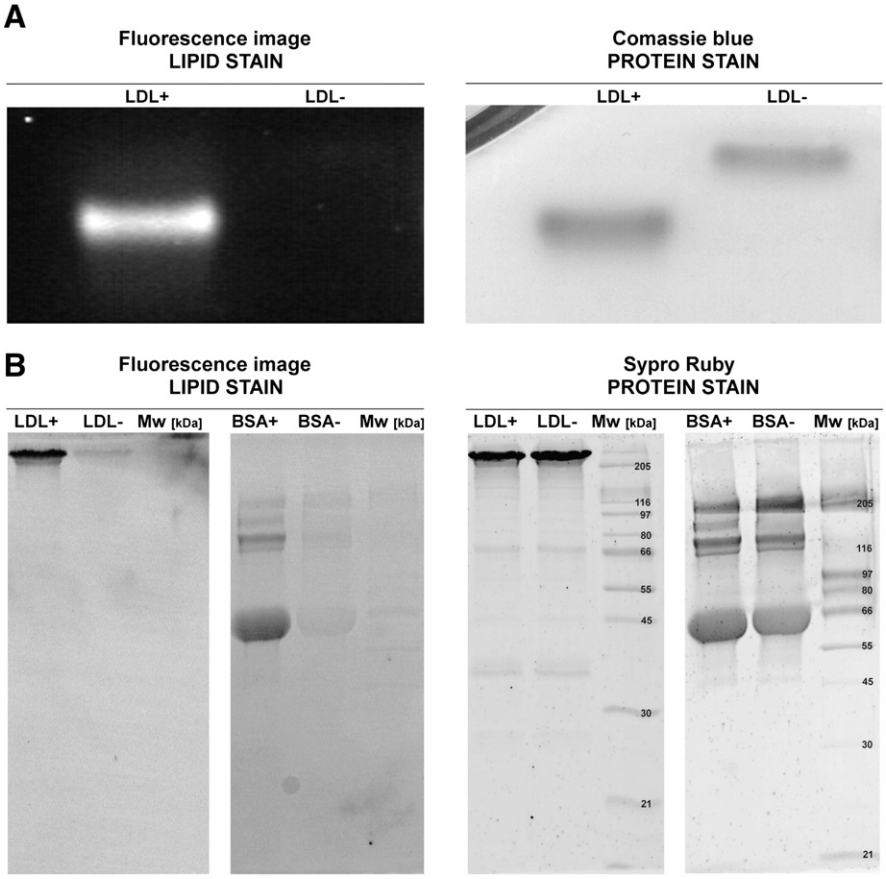

Fig. 2. Characterization of molecular and supramolecular carriers of BY-POVPE (+ represents complexes labeled with BY-POVPE; − represents unlabeled references). Panel A. Agarose gel electrophoresis (0.5%) of labeled LDL. LDL/BY-POVPE complexes (20/1, mol/mol; 5 μM label) show uniform bands with higher mobility of the labeled particle which is due to a more negative net charge as a consequence of covalent modification of amino groups by the aldehydo lipid. Panel B. SDS-PAGE of labeled LDL and BSA: LDL/BY-POVPE complexes (20/1, mol/mol; 5 μM label) and BSA/BY-POVPE complexes (1/1, mol/mol; 5 μM label) show stable labeling of LDL protein and BSA by the aldehydo lipid. Fluorescent images were obtained using a Herolab imager (panel A) or a BioRad laser scanner (panel B).

chain oxidized phospholipids leading to polar degradation products partitioning more efficiently into the aqueous phase [25]. Exposure to the fluorescent oxPL analogs leads to slightly different cell sizes and morphologies which is due to the different modes of lipid–cell interactions. The aldehydophospholipid chemically binds to its molecular targets, whereas the carboxylate lipid does not.

Despite the fact that the lipid aldehyde BY-POVPE is firmly bound to LDL and albumin, it is released from these carriers to the phospholipids and proteins of the cell plasma membrane suggesting high reversibility of Schiff base formation. This observation prompted us to study the transfer of the aldehydophospholipid between the individual donor systems LDL and albumin on the one hand and the release of cellular phospholipid to albumin on the other hand. Fig. 4A shows that BY-POVPE can be transferred from labeled LDL to unlabeled albumin in a concentration-dependent manner. After incubation of both "donor" systems followed by SDS electrophoresis, the fluorescence can be seen both in the apoB and the albumin band. The emission intensity correlated with the amount of albumin in the incubation mixture. Release of BY-POVPE from LDL is significantly reduced after treatment with $NaCNBH_3$ leading to the formation of stable amine bonds (data not shown). If cells labeled with BY-POVPE were incubated with unlabeled albumin, the same phenomenon was observed (Fig. 4B). The lipid fluorescence was detectable in the albumin band after SDS gel electrophoresis. The partitioning of the aldehydophospholipid between the different biological surfaces would be in line with the assumption that a significant fraction of the imines in the protein–lipid complexes is protonated and therefore prone to nucleophilic attack by other amines in the sample. In the literature, a pK value around 7 has been reported for aliphatic Schiff bases [26]. The accurate pK values of the imine groups in POVPC conjugates with the target proteins found in this study are unknown and have to be determined. They may vary depending on the individual protein component.

We isolated and identified the protein targets of BY-POVPE in cultured macrophages, which are expected to form covalent Schiff base adducts (Fig. 5). Because the imine complexes are unstable, they have to be stabilized before isolation and separation by chemical reduction leading to the formation of the stable amines. We used a proteome approach to identify the lipid binding proteins in total cell lysates as well as in the total membrane fractions. For this purpose, the cells were incubated with the fluorescent lipid, followed by lysis and isolation of total membranes by centrifugation. Proteins of total cell lysates were separated by 2-D PAGE (Fig. 6A), whereas the total membrane fraction was subjected to 1-D SDS electrophoresis (Fig. 6B). The fluorescent protein spots/bands were excised and tryptically digested followed by MS/MS analysis of the peptides. Fig. 6A and B show that the fluorescence patterns reflecting the labeled protein targets are much less complex than the total protein patterns detected after SYPRO Ruby™ staining. Obviously, the protein targeting by the oxidized phospholipids is selective rather than random. This effect may be due to the different pK values of differently exposed amino groups and steric constrains as a consequence of different lipid–protein and protein–protein interactions in the membrane. The specific protein targeting by BY-POVPE is underscored by the data shown in Fig. 6B. The fluorescence image shows the protein targets of the phospholipid aldehyde in membranes depending on

fluorophore concentration in the incubation medium. Higher lipid concentrations lead to uniformly higher fluorescence intensities of the individual bands, but the fluorescence pattern is always the same. Obviously, protein modification by BY-POVPE is a selective process. According to the data in Tables 1 and 2, it affects polypeptides involved in membrane transport (*e.g.* VDAC), stress response (*e.g.* heat shock proteins), apoptosis (*e.g.* cathepsin D, caspases) and lipid metabolism (*e.g.* N-acyl-sphingosine hydrolase) (Tables 1 and 2). In the membrane fraction and especially in the total cell lysate, we do not only find membrane but also cytosolic proteins. These targets may be labeled by a small fraction of lipid entering the cell interior. Once a cytosolic protein is alkylated by the aldehydophospholipid, it becomes associated with lipid bilayers and, as a consequence, shows up in the membrane pellet after ultracentrifugation.

In order to find out whether the protein complexes of fluorescent BY-POVPE reflect the interactions of unlabeled POVPC, competition experiments were performed (Fig. 7). Bovine serum albumin (panel A) or cultured RAW 264.7 cells (panel B) were incubated with mixtures of BY-POVPE and POVPC. Fluorescence labeling of albumin was suppressed by POVPC in a concentration-dependent manner. Fluorescence labeling of protein targets in live cells was also abolished by the unlabeled lipid. It seems that the fluorescence of BY-POVPE is less easily suppressed by POVPC in albumin than in RAW cell proteins at the same ratio of labeled to unlabeled lipid. It remains to be clarified why this protein and presumably other isolated proteins are modified by amphipathic lipid aldehydes to a different extent as compared to polypeptides in the complex (supra)molecular environment of live cells. We conclude that fluorescently labeled BY-POVPE is a useful analog of POVPC. This assumption is also supported by findings of other laboratories (see Discussion).

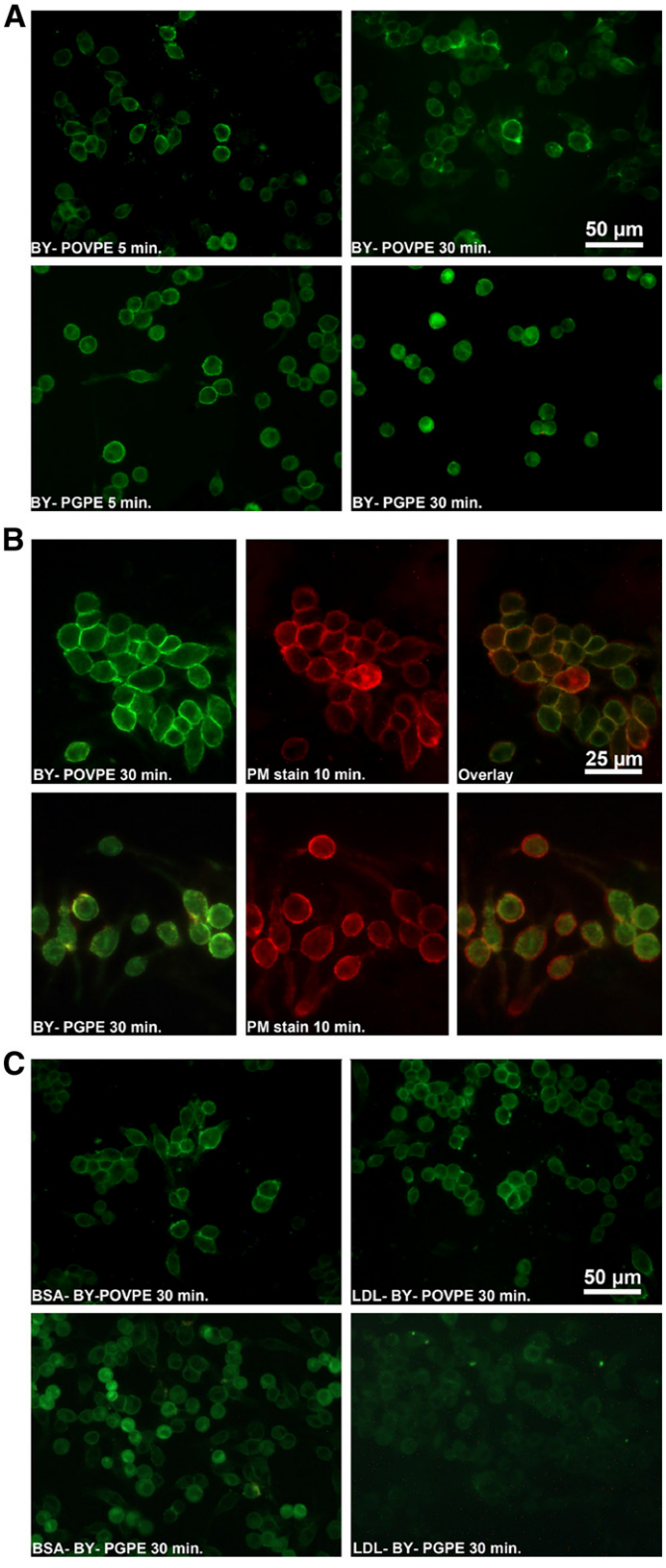

Fig. 3. Uptake of oxPLs by RAW 264.7 macrophages from different carriers. Panel A: Fluorescence micrographs (320×) of RAW 264.7 cells incubated with oxPL (5 µM) suspensions in PBS over 5 and 30 min. BY-oxPLs fluorescence is detected in the plasma membrane after 5 min incubation time. BY-PGPE is rapidly internalized by the cells. In contrast, BY-POVPE stays much longer in the plasma membrane due to formation of covalent adducts with free amino groups of proteins and lipids. Panel B: Image section of fluorescence micrographs (320×) of RAW 264.7 macrophages incubated with fluorescent oxPL (10 µM, suspension in PBS). After incubation cells were stained with Cellmask Deep Red plasma membrane (PM) stain (5 µg/ml in PBS) for 10 min. BY-POVPE, but not BY-PGPE colocalized with the plasma membrane stain. Panel C: Fluorescent micrographs (320×) of RAW 264.7 cells pre-incubated with BY-oxPL labeled BSA or LDL for 30 min. Similar patterns are found for oxPL uptake from different carriers. In case of BY-POVPE most of the fluorescence is detected in the plasma membrane where the fluorescent POVPC analog is captured by proteins and lipids. Only low amounts of the fluorescent PGPC analog are taken up by the cells from LDL or mmLDL. These low apparent uptake efficiencies are due to prior oxPL degradation in the lipoprotein. No autofluorescence was detected in unlabeled control cells.

4. Discussion

Sustained exposure of cultured vascular cells to the truncated oxidized phospholipids PGPC and POVPC leads to apoptotic cell death. A couple of receptors have so far been discussed as primary signaling platforms propagating the toxic lipid effects. Since both compounds are structurally related to platelet activating factor (PAF), they show binding affinities for the PAF receptor [27]. Other receptor candidates have also been suggested including TLR-2 and CD 36 [28]. The latter protein preferably binds lipid or protein domains with net negative charges and therefore is a receptor candidate for PGPC. This assumption is underlined by the Whisker model suggested by Greenberg et al. [29]. According to this hypothesis, oxidized phospholipids mainly influence the properties of membrane surfaces via their polar acyl chains which protrude into the aqueous phase. This assumption has meanwhile been supported by molecular dynamic studies by Khandelia and Mouritsen on Paze-PC and Poxno-PC that are longer chain homologs of PGPC and POVPC, respectively [9].

Although many cellular effects of oxidized phospholipids are mediated by receptors it is unlikely that specific receptor binding is the only primary event responsible for lipid activity. In contrast to water-soluble peptides or small molecules as receptor ligands, (oxidized) phospholipids are amphipathic and as a consequence easily partition into the plasma membrane bilayer where they can elicit signaling effects on the molecular and supramolecular level. On the one hand, they can undergo bimolecular interactions with several proteins (enzymes) or, on the other hand, perturb a larger membrane

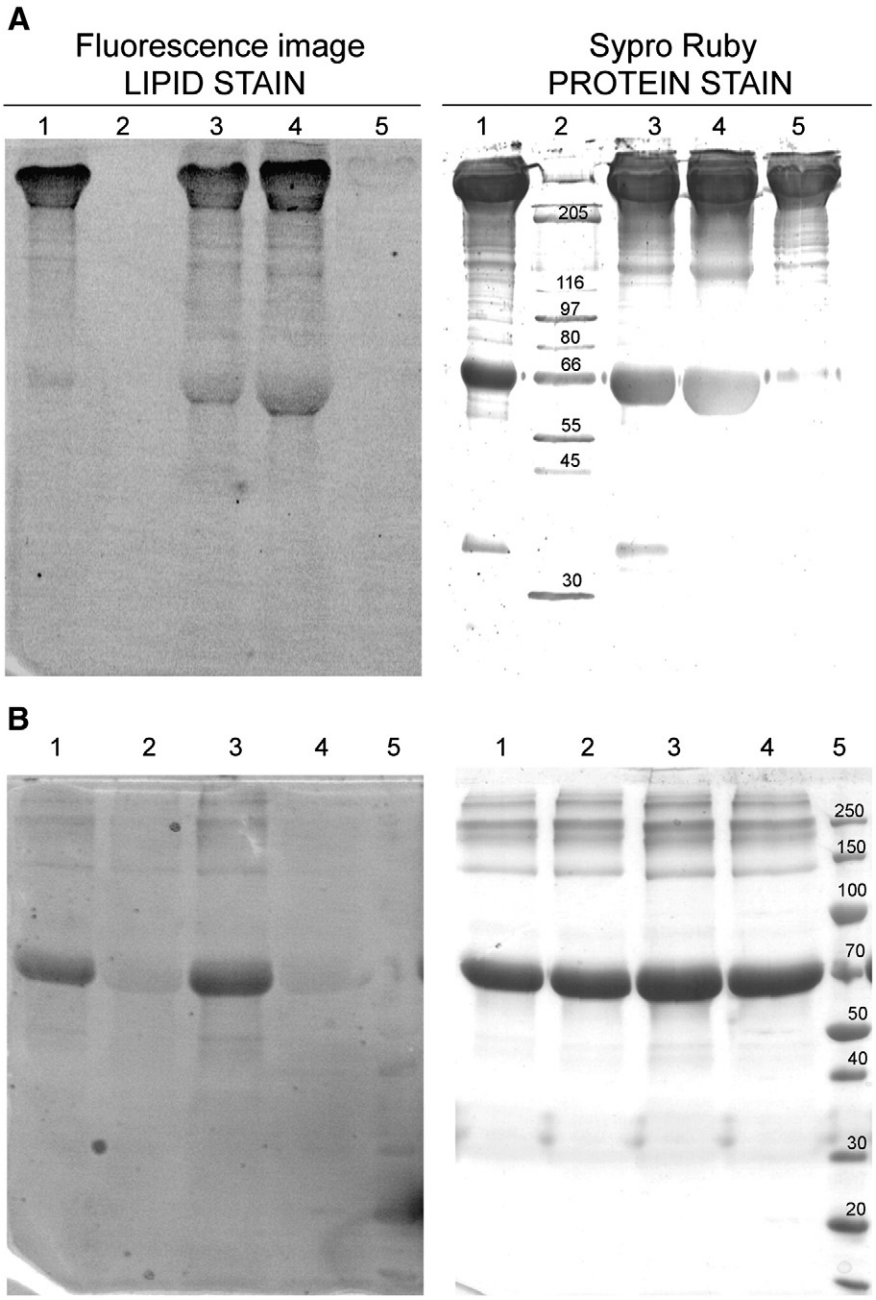

Fig. 4. Transfer of BY-POVPE between lipid donors — reversibility of Schiff base formation in BY-POVPE-protein complexes. Panel A: LDL/BY-POVPE complexes were incubated with various amounts of BSA followed by protein separation using SDS-PAGE. Fluorescence imaging of labeled lipid–protein complexes on SDS gels shows that BY-POVPE is transferred from LDL to bovine serum albumin in a concentration-dependent manner, indicating that Schiff base formation between BY-POVPE and its targets is reversible. LDL has a higher capacity than BSA for accommodating BY-POVPE (apoB and phospholipid monolayer). BY-POVPE exchange between the following systems was studied (mol LDL refers to the molar amounts of apoB100). Lane 1: LDL-BY-POVPE: BSA 1:1 mol/mol; lane 2: MW standard; lane 3: LDL-BY-POVPE: BSA 1:5 mol/mol; lane 4: LDL-BY-POVPE: BSA 1:10 mol/mol; lane 5: LDL reference. Panel B: RAW 264.7 cells were incubated with BY-POVPE (10 μM) or without label (blank sample) for 15 min followed by extensive washing with PBS and adding of 10 μM BSA solution. This mixture was incubated for 15 min. The BSA containing supernatant of BY-POVPE treated (lanes 1 and 3) or blank samples (lanes 2 and 4) was collected and split into two aliquots. One sample was incubated under reducing conditions for 30 min to stabilize the Schiff base. The proteins were precipitated and separated by SDS gel electrophoresis prior to detection of fluorescence by laser scanning and protein staining with Coomassie blue. Without reductive stabilization of the Schiff base the same results were obtained, but the fluorescence intensities were much weaker. Lanes 1 and 2: 20 μg protein; lanes 3 and 4: 40 μg protein; lane 5: MW standard. Lanes 1 and 3 show that BY-POVPE is back-transferred from the cell surface to BSA. Fluorescence intensities depend on lipid acceptor concentration. The slight autofluorescence of BSA in lanes 2 and 4 is due to the emission of bound bilirubin.

area thus activating a series of proteins in a more unspecific manner. Sustained protein activation can be evoked by the phospholipid aldehyde POVPC. This compound alkylates proteins by Schiff base formation thereby improving their association and interaction with membrane bilayers. Typical functional consequences have already been demonstrated by Kinnunen and colleagues. They found that Poxno-PC, a longer chain homologue of POVPC, improved phospholipase A2 activity in artificial membranes and abolished the lag time that is usually observed with interfacially active enzymes [30]. Other aldehydes have also been shown to activate membrane proteins in a covalent manner. For instance, modification of the epidermal growth factor receptor by hydroxynonenal mimics binding of its natural ligand thereby triggering specific signaling cascades [31,32]. Finally, plasma membrane-bound oxidized phospholipids may be released inside the cells where they can influence a number of other proteins/enzymes directly.

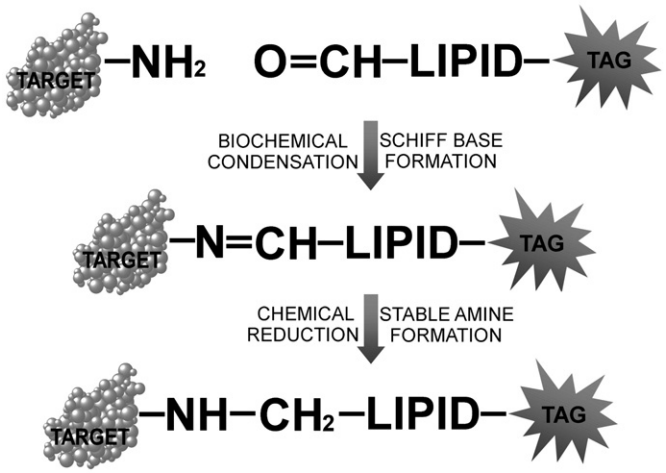

Fig. 5. Covalent interaction of POVPC with protein and lipid targets.The aldehyde group at the truncated *sn*-2 chain of POVPC forms a covalent Schiff base with free amino groups of proteins and presumably aminophospholipids (PE and PS). Since Schiff bases are unstable, the imines are chemically reduced to the stable amines for further analysis.

Truncated phospholipids contain only one long hydrophobic fatty acid. As a consequence, they are highly exchangeable between lipid–water interfaces. Therefore, it is likely that the biological activities of PGPC and POVPC are due to multiple lipid–protein or lipid–lipid interactions rather than specific binding to a couple of receptors. In this study, we used fluorescently labeled derivatives of PGPC and POVPC to measure lipid uptake into cultured RAW 264.7 macrophages and identify their primary protein targets. The fluorescent lipids contained a BY-fluorophore bound to the polar head groups. They are reliable analogs of their natural counterparts. It has already been shown by the group of Berliner that the biological activities of truncated phospholipids are mainly determined by the structure of the polar *sn*-2 acyl chain and to a much lesser extent by the structure of the polar heads [33]. We found that proper labeling of oxidized phospholipids did not significantly alter their signaling effects. Head group-labeled analogs and unlabeled lipids elicited the same activation of acid sphingomyelinase generating the apoptotic lipid messenger ceramide [8,11]. A comparative study on the inflammatory response of vascular cells towards oxidized phospholipids and their biotin-labeled analogs also provided evidence that head-group labeling is not critical [34]. All these observations are in agreement with the assumption that the truncated oxidized phospholipids mainly "communicate" at the membrane surface via their polar *sn*-2 acyl chains (see above).

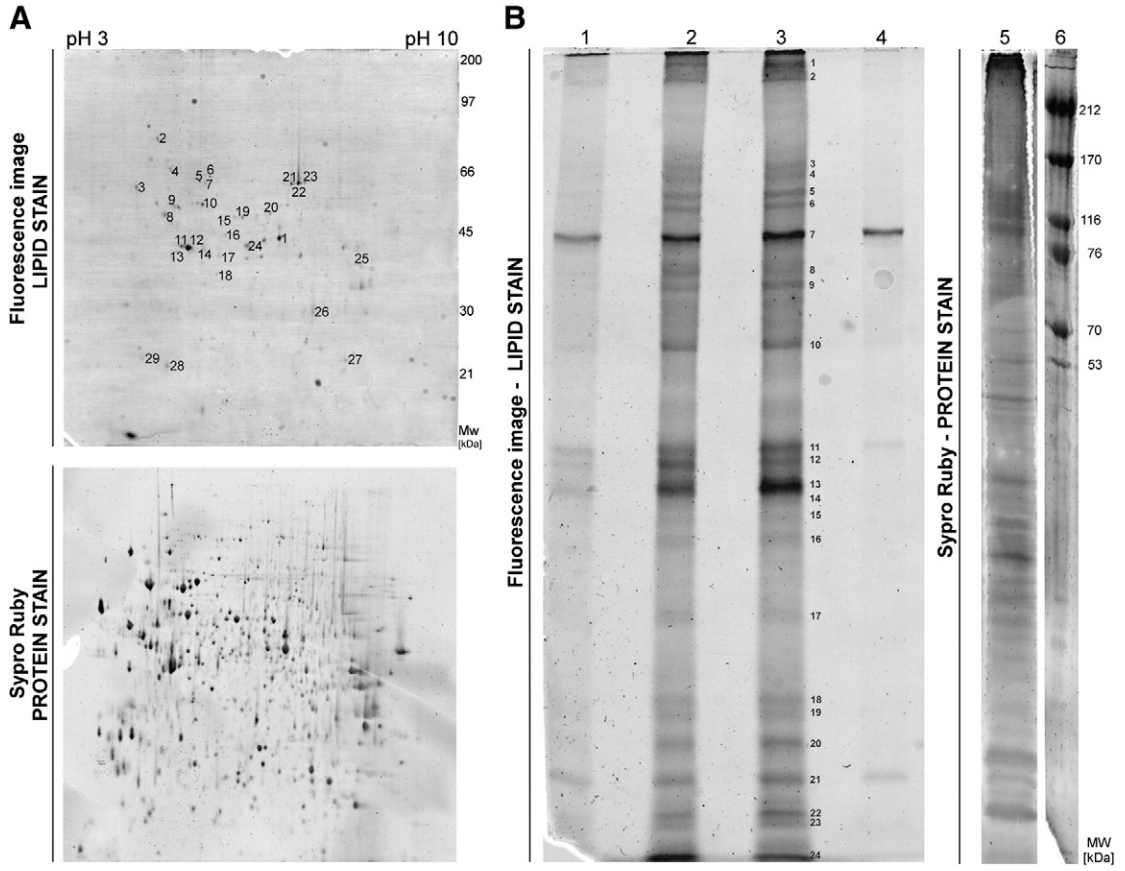

Fig. 6. Protein targets of fluorescent BY-POVPE in RAW 264.7 macrophages.Panel A: Cells were incubated with BY-POVPE (10 μM) in PBS for 30 min followed by lysis under reductive conditions to stabilize the lipid–protein complexes (Schiff bases). The labeled proteins were precipitated and separated by 2-D SDS gel electrophoresis. Fluorescent proteins were imaged using a fluorescence laser scanner (BioRad). The lipid stain represents the proteins covalently attached to the fluorescent oxPL. The SYPRO Ruby™ stain represents the full cell proteome. The fluorescence patterns show that the staining of the protein targets by BY-POVPE is a selective process affecting only a defined subset of the cell proteome. Panel B: Cells were incubated with different concentrations of BY-POVPE in PBS over 30 min followed by separation of the membrane fraction using ultracentrifugation ($>100{,}000\times g$). The membrane pellets were isolated and resuspended in PBS prior to protein precipitation and separation by 1-D SDS gel electrophoresis. After incubation of the cells with the oxPL, all procedures were performed under reductive conditions (see above). Fluorescent proteins were imaged using a fluorescence laser scanner (BioRad). The lipid stain represents the proteins covalently attached to the fluorescent oxPL. BY-POVPE concentrations in the incubation mixtures: lane 1: 1 μM; lane 2: 2.5 μM; lane 3: 5 μM; lane 4: 0 μM, shows only autofluorescent proteins; lane 5: SYPRO Ruby™ full protein stain of one representative lane, lane 6: MW standard. Fluorescence intensities of the BY-POVPE-labeled protein targets depend on lipid concentration and leveled off at 5 μM lipid. The fluorescent patterns and therefore the selectivity of labeling were unaffected by the amount of BY-POVPE.

Table 1
Protein targets of BY-POVPE in total RAW 264.7 macrophage lysates. Highlighted proteins have also been found in the membrane fractions (Table 2). Cells were incubated with BY-POVPE (10 μM) in PBS for 30 min followed by lysis and 2-D SDS gel electrophoresis. Spots (Fig. 6 panel A) were excised and tryptically digested. Subsequently, peptides were analyzed by MS/MS and targets were identified by database search (NCBI, Expasy, SwissProt, Brenda).

Spot (#)	Spectra (#)	Distinct Peptides (#)	Distinct Summed MS/MS Search Score	AA Coverage [%]	Protein MW [Da]	Protein pI	Database ID Accession GI (#)	Protein Name
1	8	5	49.09	11	46798.50	5.97	26347479	sorting nexin 5
1	12	4	44.93	11	45771.10	6.23	148709540	leupaxin
2	154	25	384.54	35	92490.30	4.74	14714615	Heat shock protein 90kDA beta (Grp94)
3	8	4	53.45	10	48021.80	4.34	74227675	calreticulin
4	467	32	550.23	53	72422.40	5.07	2506545	78kDa glucose reulated protein precursur
5	173	20	336.08	36	70947.50	5.37	74198978	Dank-type molecular chaperone hsp72-ps1
5	37	10	158.11	19	72416.70	5.83	74192747	arginyl aminopeptidase
6	255	14	246.43	26	73528.70	5.91	6754256	heat shock protein 9 grp 75 Hsp709A
7	371	24	400.41	44	70947.50	5.37	74198978	Dank-type molecular chaperone hsp72-ps1
7	34	7	122.94	14	68368.50	5.42	31560731	ATPase. H+ transporting. lysosomal V1 subunit A
8	9	3	48.82	11	39370.90	4.95	148686207	lymphocyte specific 1
9	14	8	134.39	16	72477.50	5.10	2598562	BiP Hsp70 protein GRP78
9	6	3	40.65	6	57079.20	5.88	149023098	protein disulfid isomerase associated 3
10	70	14	190.29	31	56775.30	5.89	148691054	ubiquitin- specific peptidase 14
10	65	13	185.40	27	61054.90	6.07	51766670	heat shock protein 1 (chaperonin)
10	14	4	46.81	6	58928.90	5.48	74214557	copine I
11	202	7	120.29	21	45002.10	5.42	148673963	mCG13192 p47 protein
12	11	5	66.67	16	38358.20	5.17	6754910	mCG19035, nudC nuclear distribution gene C
12	3	2	22.20	4	53711.20	5.12	74184979	ataxin10
13	7	5	64.87	19	37402.30	5.06	7305121	glycogenin
14	21	7	111.06	21	38358.20	5.17	6754910	mCG19035. nudC nuclear distribution gene C
15	10	3	46.74	8	45565.50	5.86	74212703	RasGAP-associated protein p56dok-2
16	67	13	202.10	31	51146.80	5.49	70794778	RuvB-like 2
16	22	4	64.72	12	48374.20	6.85	26354406	cathepsinD
17	12	4	53.33	12	393514.00	5.44	27370510	paraoxonase3
17	5	2	35.39	6	37719.60	5.61	148683063	guanine nucleotide binding protein
18	3	3	33.73	10	35930.00	5.43	33416530	Annexin A4
19	27	11	139.71	26	51777.80	5.58	18017596	sorting nexin 4
19	50	10	133.75	20	57538.20	5.57	74191447	vacuolar H+ATPase B2
20	43	9	120.41	19	56585.90	8.30	5235955	3-phosphoglycerate dehydrogenase
21	13	5	66.45	9	72613.90	7.06	74219241	succinate dehydrognease Fp subunit
22	59	6	75.52	11	60630.40	6.28	6753320	chaperonin subunit 3
22	123	4	56.40	7	72613.90	7.06	74219241	succinate dehydrognease Fp subunit
23	75	12	203.43	24	75801.50	8.30	148704343	phosphoenolpyruvate carboxykinase 2
23	8	4	52.80	7	72613.90	7.06	74219241	succinate dehydrognease Fp subunit
24	4	2	26.11	5	46762.20	5.86	148704797	sorting nexin 6
24	11	6	83.96	15	45640.70	5.73	86198305	caspase1
25	3	2	25.95	5	44669.80	8.86	9790019	N-acyl sphingosine amidohydrolase
26	22	6	88.00	22	31746.00	7.44	33243895	voltage dependent anion channel2 VDAC-2
26	10	3	41.70	16	31475.00	6.46	6753284	caspase3
27	8	3	42.05	16	22236.70	8.26	12846314	peroxiredoxin1
28	5	2	29.80	6	36856.50	4.72	7106546	LOC298795 protein, similar 14-3-3 sigma
29	14	4	65.88	15	29965.70	8.25	74185553	Tat-interacting protein TIP30
29	3	2	30.52	7	32577.80	7.67	74212025	voltage dependent anion channel VDAC-1

Since we used fluorescent PGPC and POVPC analogs, we were able to study the time-dependent lipid uptake and localization in live cells reducing the probability of artefacts. In a previous study on the import of biotin-tagged oxidized phospholipids into HAEC, cell fixation was required for lipid localization by secondary fluorescence staining of biotin [34]. This stabilization is based on cross-linking by aldehydes which affects and perturbs (subcellular) membrane assemblies.

In agreement with previous studies, the fluorescent PGPC analog was quickly internalized by the cells [24]. In contrast, POVPC was retained in the plasma membrane since it contains an aldehyde group which can form covalent Schiff bases with the amino groups of proteins and phospholipids. It is striking, especially in the case of POVPC, that delivery of the labeled phospholipids analogs to the cells did not depend on the lipid donor (aqueous lipid dispersions and lipid complexes with albumin and LDL).

Lipid complexes with albumin and LDL are likely to be physiologically relevant donors of oxidized phospholipids *in vivo*. LDL is a site of lipid oxidation. Albumin may extract oxidized phospholipids from the particle, since it shows binding affinities for phospholipids containing only one long hydrophobic fatty acid, *e.g.* lysolecithin [23]. We were able to show that both carriers form stable complexes with fluorescent oxidized phospholipids also (Fig. 2). Whereas PGPC only physically binds to proteins and lipoproteins, POVPC is covalently linked to these carriers. However, regardless of covalent binding, the POVPC analog is released from these donor systems to cells and *vice versa*. In addition, it is freely exchangeable between the individual donors. This exchangeability is due to the instability of the covalent lipid adducts. The pK-values for Schiff bases around 7 [26] make the imines prone to protonation and nucleophilic substitution by other amines. As a consequence, short-chain oxidized phospholipids, including phospholipid aldehydes, are not only active at the site of their formation but can be spread as "signal transducers" to the near cellular environment by diffusion within the tissues as well as to tissues far distant from the site of oxidative stress via the circulation. The relevance of such processes has already been underscored by the identification of small particles in the circulation that are enriched in oxidized phospholipids [35,36].

We screened for the primary protein targets of aldehydophospholipids in cultured macrophages using a fluorescent POVPC analog. This phospholipid forms covalent Schiff bases that can be stabilized by chemical reduction for further protein separation, detection and analysis. In contrast to our "expectations", protein labeling by this compound was selective (Fig. 6). A fluorescence image of the phospholipid-tagged

Table 2
Protein targets of BY-POVPE in the total membrane fraction of RAW 264.7 macrophages. Membrane-associated proteins are highlighted. Cells were incubated with BY-POVPE (5 μM) in PBS for 30 min followed by the isolation of the total membrane fraction and 1-D SDS gel electrophoresis of the proteins. Bands (Fig. 6 panel B) were excised and tryptically digested. Subsequently, peptides were analyzed by MS/MS and targets were identified by database search (NCBI, Expasy, SwissProt, Brenda).

Band (#)	Spectra (#)	Distinct Peptides (#)	Distinct Summed MS/MS Search Score	AA Coverage [%]	Protein MW [Da]	Protein pI	Database ID Accession GI (#)	Protein Name
1	68	20	328.08	5	534218.4	5.74	122065897	Plectin-1
1	56	18	293.94	4	532048.3	6.03	134288917	dynein, cytoplasmic, heavy chain-1
2	138	21	357.47	10	272134.3	5.92	49022858	talin 1, isoform CRA_b
2	25	5	81.7	2	274938.7	6.16	148702862	fatty acid synthase, isoform CRA_b
2	3	2	25.43	1	125954.4	6.92	148704174	ATPase, aminophospholipidtransporter-like, class I
3	47	10	149.35	14	92771.4	4.72	14714615	rCG49111- Hsp90kDa beta (Grp94), member1
3	49	7	107.49	9	113054.9	5.30	6978543	ATPase, Na+/K+ transporter, alpha1 polypeptide
3	30	15	253.46	17	123093.4	5.72	38604071	exportin
3	14	3	55.49	4	91048.2	5.26	148670554	valosin
3	3	2	36.05	4	85026.4	7.02	3183523	Integrin beta 2 precursor
4	33	7	114.46	11	84816.3	4.93	74147335	heat shock protein 1. alpha
4	29	12	203.06	21	67278.3	4.50	6671664	calnexin
5	140	28	482.63	45	83341.8	4.97	51859516	Hsp90
5	22	11	184.59	17	86295.4	7.02	148666539	inner mebrane protein
5	19	7	97.68	15	53748	5.06	74199770	vimentin
6	28	9	142.87	12	86295.4	7.02	148666539	inner membrane protein , mitochondrial
7	80	25	440.32	39	74300	6.54	12835914	Lamin A isoform A
7	39	16	277.7	28	70208.7	5.12	74139671	lymphocyte cytosolic protein 1
7	36	15	248.36	31	74570	8.43	27369581	solute carrier family 25
7	51	14	240.71	25	72613.9	7.06	74219241	succinate dehydrogenase Fp subunit
7	13	6	94.56	11	70947.5	5.38	74198978	Dank-type molecular chaperone hsp72-ps1
7	9	4	59.81	7	68528.7	6.02	48474583	Dolichyl-diphosphooligosaccaride-protein GT
7	7	2	32.39	4	71376.8	7.92	56550045	spleen tyrosin kinase
7	3	3	36.85	4	70208.7	5.12	7413967	65-kDa macrophage protein
7	2	2	26.97	3	69311.5	5.73	50510565	SWA-70 protein
8	262	28	500.67	62	57846.2	6.66	74221210	pyruvate kinase
8	29	11	199.54	27	59684.6	7.95	74151643	T-complex protein 1 subunit
8	22	14	218.65	28	58104.7	6.46	74204595	chaperonin subunit 6a
8	19	9	125.33	18	53748	5.06	74199770	vimentin
8	18	5	80.47	9	58084.7	8.24	74204209	chaperonin subunit 4 (delta)
8	13	8	123.87	19	56678.7	5.88	112293264	protein disulfid isomerase associated 3
8	6	2	30.56	4	57079.2	5.88	149023098	protein disulfid isomerase associated 3
8	5	3	41.14	8	57987.6	5.37	31543458	p21-activated kinase 2
9	165	18	343.58	49	56667.1	5.24	23272966	Atp5b protein
9	302	32	563.07	65	53687.9	5.06	31982755	vimentin
9	76	17	312.48	50	53811.8	8.10	148698452	CAP, adenylat cyclase-associated protein 1
9	72	17	244.43	36	53688.9	5.04	74139645	vimentin
9	62	19	345.6	53	57477.6	5.97	126521835	chaperonin subunit 2
9	53	17	300.52	38	59766.9	9.22	74211072	ATP synthase, H+ transporting
9	22	10	186.6	27	57538.2	5.58	74191447	vacuolar H+ ATPase B2
9	12	5	74.71	8	65442.5	9.27	50510859	sphingosine phosphate lyase
9	3	2	27.37	5	54305.1	8.28	16758554	phosphadidylinositol 4-kianse type2 alpha
10	18	5	74.8	12	51737	8.72	13385942	citrate synthase
10	10	3	54.98	11	48374.2	6.86	26354406	cathepsin D
11	232	5	82.95	18	33312.5	9.83	61556754	prohibitin 2
11	101	4	72.92	17	31746	7.44	13786202	voltage dependent anion channel 2
12	84	5	87.14	22	32351.6	8.55	10720404	voltage dependent anion channel 1
12	33	5	85.21	18	35148	7.60	74207645	guanine nucleotide binding protein
13	86	8	122.73	26	32931.5	9.74	22094075	solute carrier family 25, member 5
13	27	9	149.32	31	35096.8	5.36	74215924	14-3-3 gamma
13	12	6	118.01	33	29087.8	4.71	148676868	14-3-3 zeta
13	9	5	85.39	25	30884.1	8.96	5980769	voltage dependent anion chanel 3
13	8	2	38.55	11	25067.2	6.10	123234567	tumor protein D52-like 2
14	15	3	38.22	8	31611.1	9.20	148697937	B-cell receptor- associated protein 31
15	30	3	57.65	11	32191.9	5.57	148667347	Triphosphatisomerase
15	30	2	39.68	10	26927.2	4.92	70608194	tumor protein D52-like 2
16	22	2	41.4	12	31440.6	6.54	975689	stomatin
16	20	3	45.81	13	23927.1	5.85	16758368	RAB 14, member Ras oncogen family
17	15	5	92	25	22541.1	8.58	7710086	RAB 10, member Ras oncogen family
17	7	2	25.36	7	28144.9	9.55	148687100	RAS-related C3 botulinum substrate 1
18	320	4	54.53	16	20246.8	11.39	30061401	histone cluster 2, H3c1 isoform 2
18	42	3	53.13	28	11651	4.42	83745120	ribosomal protein, large P2
19	461	6	96.76	40	16572.4	10.13	149029297	histone 1, H2bn
19	127	3	59.3	30	14759	9.21	6677775	ribosomal protein L22
20	54	2	38.49	15	17748.7	10.85	149263957	ribosomal protein S18
21	152	5	90.57	32	17239.2	10.59	94378251	similar to histone 4
22	11	2	32.61	21	9326.8	9.52	33563266	NADH dehydrogenase 1 alpha subcomplex
23	58	2	35.12	21	9326.8	9.52	33563266	NADH dehydrogenase 1 alpha subcomplex
24	8	3	44.93	5	56505.3	5.10	57012436	keratin 10

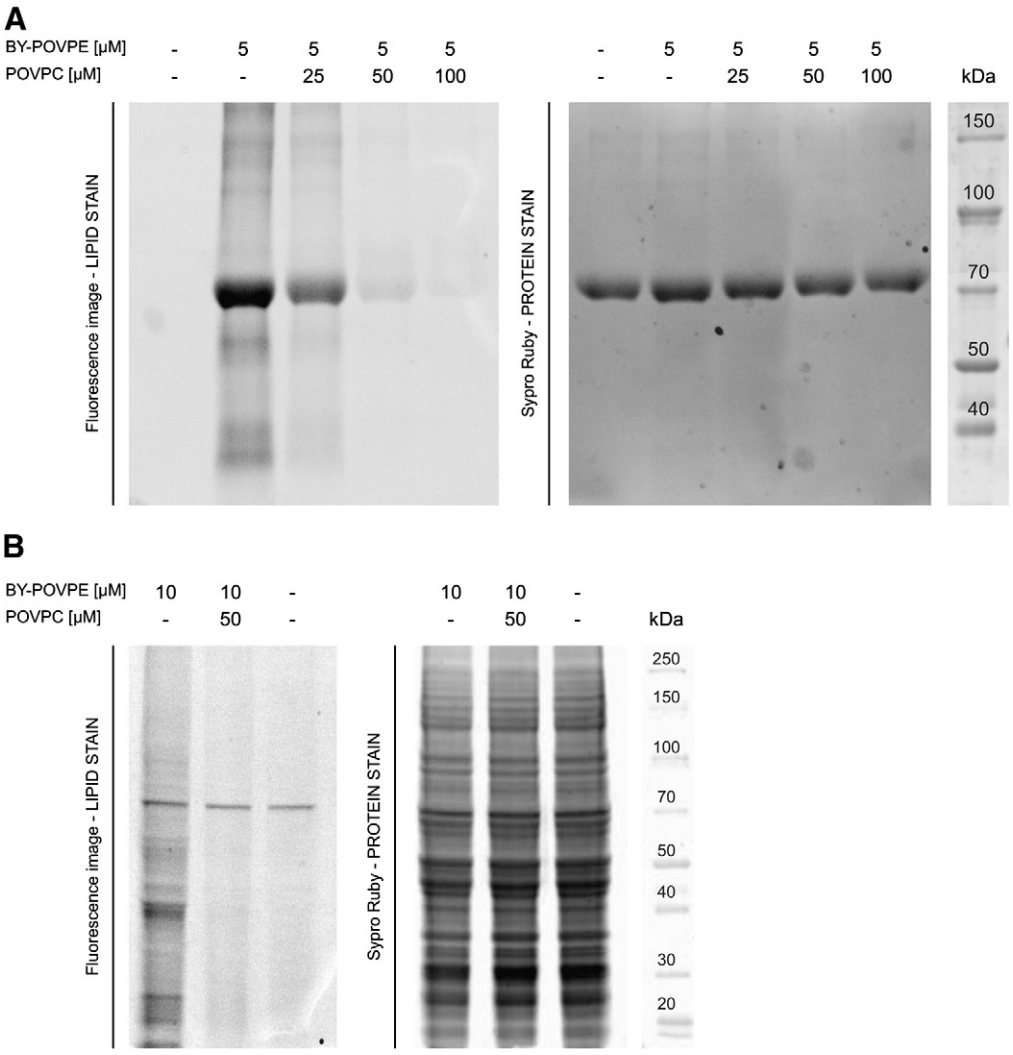

Fig. 7. Inhibitory effect of POVPC on Schiff base formation of BY-POVPE with proteins.Incubation of albumin and RAW cells with BY-POVPE-POVPC mixtures, isolation and separation and fluorescence detection of labeled proteins were performed as described in the Materials and methods section. Shown are the fluorescence images of labeled proteins after SDS gel electrophoresis. Lipid stain: fluorescence of proteins labeled with BY-POVPE. Total protein stain: fluorescence of protein-bound SYPRO Ruby™. Panel A: fluorescence labeling of albumin. Panel B: fluorescence labeling of RAW cell proteins. In both cases, unlabeled POVPC suppresses protein labeling by BY-POVPE.

proteins was much less complex than a total protein stain of the same cell lysate. A similar observation was made with a biotin-tagged oxidized phospholipid mixture in HAECs [34]. We suppose that this selectivity is not due to specific molecular recognition but rather due to differences in the pK values of the individual amino groups of the target proteins. This value is influenced by surface exposure and interaction with membrane lipids and proteins in the immediate vicinity. A detailed analysis of the labeled target candidates led to the identification of proteins involved in cell death and survival, stress response, transport and lipid metabolism. There is some overlap between the protein targets detected by the biotin-tagged probes [34] and the fluorescent POVPC analog. However, many other proteins identified in our studies have not been reported in literature so far.

Protein modification by POVPC may lead to activation of apoptotic signaling components, as well as suppression of functions that help the cell survive. Here, we would like to put the emphasis on the potential roles of some target candidates that seem particularly relevant to POVPC-induced apoptosis. Cathepsin D, caspase 1 and caspase 3 are components of programmed cell death. Cathepsin D is a lysosomal protease which is also associated with endosomal membranes [37]. Reactive oxygen species, oxidized proteins and lipids have already been shown to activate this enzyme and increase the level of p53 which is a transcription factor for cathepsin D. Activation of this protease leads to cytochrome c release from mitochondria, caspase 3 activation and cell death [38]. Heat shock protein Hsp70B is expressed and released by macrophages in response to oxidized LDL which is a carrier of oxidized phospholipids. This protein plays a key role in the activation of macrophages and helps the cells survive under oxidative stress [39]. Calcium channels have also been identified as targets of oxidized phospholipids and play a role in atherosclerosis [40]. Voltage dependent anion channel 1 (VDAC 1) is involved in mitochondria-mediated apoptosis by regulating cytochrome c release [41]. Minimally oxidized LDL rich in oxidized phospholipids induces formation of reactive oxygen species leading to proinflammatory cytokine expression. This process also depends on a target identified in this study, namely spleen tyrosine kinase. Bae et al. found that this enzyme is activated by mmLDL downstream of TLR 4 leading to ROS generation in macrophages [42]. TLR 4 signaling is inhibited by oxidized phospholipids [43], due to disruption of lipid rafts in the plasma membrane. This phenomenon is in line with results from single molecule fluorescence microscopy showing that fluorescent oxidized phospholipids (PGPC) partition into lipid raft-like membrane domains (caveolae) [24]. In this context, it is interesting to note that stomatin has also been identified as a POVPC target. This protein

belongs to a larger family of polypeptides sharing an evolutionary conserved stomatin/prohibitin/flotillin/HflK/C domain [44]. It is known from studies on epithelial cells [45], erythrocytes [46] and platelet alpha granules [47] that it is a major raft component. N-acyl-sphingosine hydrolase (ceramidase) and sphingosine phosphate lyase are also potential POVPC targets. They are involved in sphingolipid metabolism and influence the ceramide concentrations and cell susceptibility to apoptosis [48].

We and others provide evidence that head group-labeled POVPE is a reliable analog of POVPC in biological systems. Fig. 7 shows that POVPC suppresses protein modification by BY-POVPE. Moumtzi et al. found that fluorescent and unlabeled oxPL elicited the same rapid activation of acid sphingomyelinase in cultured cells. Lipid localization in the cells was the same irrespective of the lipid-bound label [11]. Gugiu et al. studied the cellular protein targets of oxidized phospholipids labeled with biotin at their head groups. They did not find any effects on biological lipid activities (competition experiments with unlabeled lipids, stimulation of interleukin 8 formation) [34]. Berliner et al. studied different oxidized phospholipid classes and found that their biological activities mainly depended on the oxidized sn-2 acyl chain, but not on the polar head group [33].

We have preliminary evidence that POVPC forms covalent adducts not only with proteins but also with aminophospholipids in cell membranes. Incubation of BY-POVPE with cultured cells led to the formation of two new fluorescent phospholipids with lower polarity. The structures of these compounds are currently subject to identification.

In summary, we have shown that fluorescent analogs of PGPC and POVPC are easily taken up into macrophages irrespective of the lipid donor. Whereas POVPC is initially scavenged by covalent reaction with the components of the plasma membrane, PGPC is quickly internalized. Despite the covalent binding to its lipid and protein targets, POVPC is freely exchangeable between membranes and (lipo-) protein surfaces. As a consequence, this lipid represents a toxic compound which is active not only at the site of its formation but also in cells far distant from areas of oxidative stress (Fig. 8). The identification of the potential POVPC protein targets supports the assumption that POVPC interacts with multiple sites and not only with the traditional specific receptors.

The proteins identified in this study are target candidates for alkylation and functional modification by the phospholipid aldehyde POVPC. It is the aim of a current project to verify the function of these proteins as primary targets and signaling platforms in macrophages under the conditions of oxidized phospholipid stress. For this purpose, we are performing gain and loss of function studies as well as FRET experiments to determine spatial lipid–protein proximity. These investigations could also help identify protein targets of the carboxylate phospholipid PGPC that cannot be found using the proteome approach described herein because this lipid does not covalently bind to other biomolecules. These studies are expected to provide new information on which target proteins represent primary signaling platforms of cell death induced in macrophages by oxidized phospholipids.

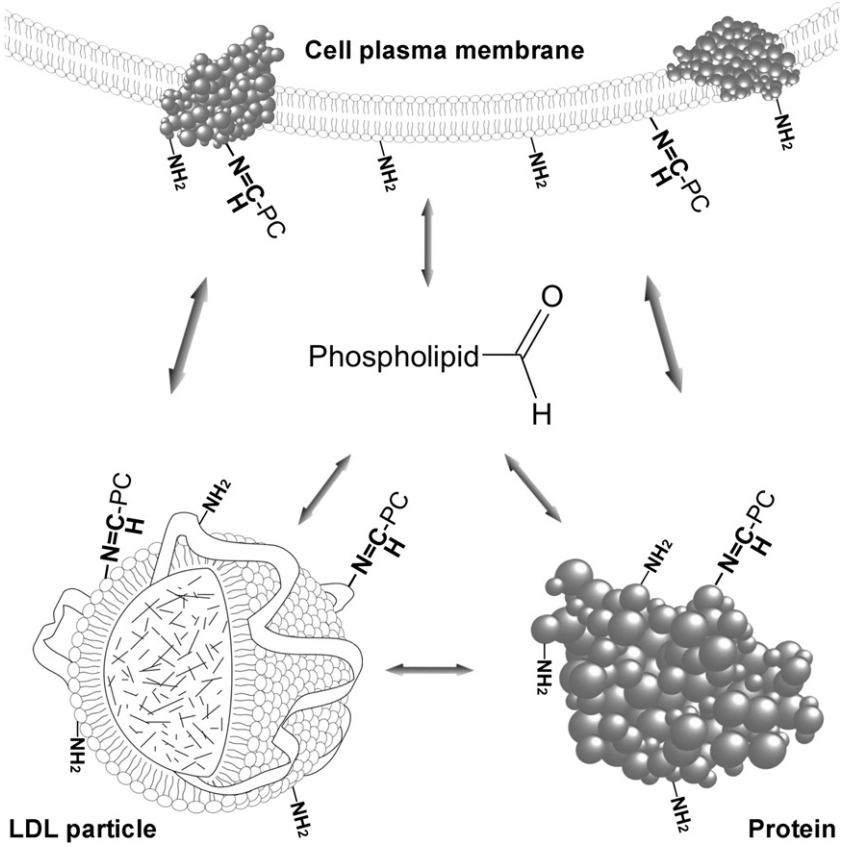

Fig. 8. Exchange of BY-POVPE between lipid–protein surfaces.OxPL, including POVPC, may be bound to at least three physiologically relevant carriers. The respective supramolecular systems are lipid aggregates (aqueous lipid suspension), complexes with proteins (BSA) and lipoproteins (LDL). POVPC forms covalent Schiff bases with the amino groups of phospholipids and proteins. Despite the fact that the oxPL is firmly bound to these molecules (see Fig. 2), it is released to lipids and proteins of the cell plasma membrane. In addition, POVPC is easily released from its albumin complex and to a lower extent from its LDL complex (see Figs. 3 and 4), too, if other lipid acceptors are present. The exchangeability of the covalently bound aldehydo lipid can be explained by the pKs of aliphatic Schiff bases around pK 7. At this pK, a significant fraction of the imine is protonated and thus subject to nucleophilic substitution by other amines. LDL showed the highest affinity for POVPC binding (accommodation in the phospholipids monolayer and binding by apoB) and can thus be considered the main carrier for delivery of the oxPL to the cells.

Acknowledgement

This work was financially supported by the Austrian Science Fund FWF (project F30-B05 — special research program SFB Lipotox) and ESF EuroMEMBRANE CRP OXPL (project I308-B12). The authors wish to thank Dr. Gholam Ali Khoschsorur (University Hospital Graz, Austria) for providing us with pooled blood plasma samples and Dr. Dagmar Kratky (Medical University, Graz, Austria) for providing the RAW 264.7 cells.

References

[1] D. Steinberg, The LDL modification hypothesis of atherogenesis: an update, J. Lipid Res. 50 (Suppl.) (2009) S376–S381.
[2] K.L. Gillotte, S. Horkko, J.L. Witztum, D. Steinberg, Oxidized phospholipids, linked to apolipoprotein B of oxidized LDL, are ligands for macrophage scavenger receptors, J. Lipid Res. 41 (2000) 824–833.
[3] H.P. Deigner, A. Hermetter, Oxidized phospholipids: emerging lipid mediators in pathophysiology, Curr. Opin. Lipidol. 19 (2008) 289–294.
[4] G.O. Fruhwirth, A. Hermetter, Mediation of apoptosis by oxidized phospholipids, Subcell. Biochem. 49 (2008) 351–367.
[5] G.O. Fruhwirth, A. Loidl, A. Hermetter, Oxidized phospholipids: from molecular properties to disease, Biochim. Biophys. Acta 1772 (2007) 718–736.
[6] A. Mertens, P. Holvoet, Oxidized LDL and HDL: antagonists in atherothrombosis, FASEB J. 15 (2001) 2073–2084.
[7] G.O. Fruhwirth, A. Moumtzi, A. Loidl, E. Ingolic, A. Hermetter, The oxidized phospholipids POVPC and PGPC inhibit growth and induce apoptosis in vascular smooth muscle cells, Biochim. Biophys. Acta 1761 (2006) 1060–1069.
[8] A. Loidl, E. Sevcsik, G. Riesenhuber, H.P. Deigner, A. Hermetter, Oxidized phospholipids in minimally modified low density lipoprotein induce apoptotic signaling via activation of acid sphingomyelinase in arterial smooth muscle cells, J. Biol. Chem. 278 (2003) 32921–32928.
[9] H. Khandelia, O.G. Mouritsen, Lipid gymnastics: evidence of complete acyl chain reversal in oxidized phospholipids from molecular simulations, Biophys. J. 96 (2009) 2734–2743.
[10] P.L. Smiley, K.E. Stremler, S.M. Prescott, G.A. Zimmerman, T.M. McIntyre, Oxidatively fragmented phosphatidylcholines activate human neutrophils through the receptor for platelet-activating factor, J. Biol. Chem. 266 (1991) 11104–11110.
[11] A. Moumtzi, M. Trenker, K. Flicker, E. Zenzmaier, R. Saf, A. Hermetter, Import and fate of fluorescent analogs of oxidized phospholipids in vascular smooth muscle cells, J. Lipid Res. 48 (2007) 565–582.
[12] B.H. Chung, T. Wilkinson, J.C. Geer, J.P. Segrest, Preparative and quantitative isolation of plasma lipoproteins: rapid, single discontinuous density gradient ultracentrifugation in a vertical rotor, J. Lipid Res. 21 (1980) 284–291.
[13] M.M. Bradford, A rapid and sensitive method for the quantitation of microgram quantities of protein utilizing the principle of protein-dye binding, Anal. Biochem. 72 (1976) 248–254.
[14] A.D. Watson, N. Leitinger, M. Navab, K.F. Faull, S. Horkko, J.L. Witztum, W. Palinski, D. Schwenke, R.G. Salomon, W. Sha, G. Subbanagounder, A.M. Fogelman, J.A. Berliner, Structural identification by mass spectrometry of oxidized phospholipids in minimally oxidized low density lipoprotein that induce monocyte/endothelial interactions and evidence for their presence *in vivo*, J. Biol. Chem. 272 (1997) 13597–13607.
[15] S. Batzri, E.D. Korn, Single bilayer liposomes prepared without sonication, Biochim. Biophys. Acta 298 (1973) 1015–1019.
[16] D. Wessel, U.I. Flügge, A method for the quantitative recovery of protein in dilute solution in the presence of detergents and lipids, Anal. Biochem. 138 (1984) 141–143.
[17] S.P. Fling, D.S. Gregerson, Peptide and protein molecular weight determination by electrophoresis using a high-molarity tris buffer system without urea, Anal. Biochem. 155 (1986) 83–88.
[18] A. Gorg, C. Obermaier, G. Boguth, A. Harder, B. Scheibe, R. Wildgruber, W. Weiss, The current state of two-dimensional electrophoresis with immobilized pH gradients, Electrophoresis 21 (2000) 1037–1053.
[19] A. Shevchenko, M. Wilm, O. Vorm, M. Mann, Mass spectrometric sequencing of proteins silver-stained polyacrylamide gels, Anal. Chem. 68 (1996) 850–858.
[20] R. Birner-Grunberger, H. Scholze, K. Faber, A. Hermetter, Identification of various lipolytic enzymes in crude porcine pancreatic lipase preparations using covalent fluorescent inhibitors, Biotechnol. Bioeng. 85 (2004) 147–154.
[21] S. Carr, R. Aebersold, M. Baldwin, A. Burlingame, K. Clauser, A. Nesvizhskii, The need for guidelines in publication of peptide and protein identification data: Working Group on Publication Guidelines for Peptide and Protein Identification Data, Mol. Cell. Proteomics 3 (2004) 531–533.
[22] A. Ravandi, A. Kuksis, N. Shaikh, G. Jackowski, Preparation of Schiff base adducts of phosphatidylcholine core aldehydes and aminophospholipids, amino acids, and myoglobin, Lipids 32 (1997) 989–1001.
[23] S.D. Brown, B.L. Baker, J.D. Bell, Quantification of the interaction of lysolecithin with phosphatidylcholine vesicles using bovine serum albumin: relevance to the activation of phospholipase A2, Biochim. Biophys. Acta 1168 (1993) 13–22.
[24] S. Rhode, R. Grurl, M. Brameshuber, A. Hermetter, G.J. Schutz, Plasma membrane fluidity affects transient immobilization of oxidized phospholipids in endocytotic sites for subsequent uptake, J. Biol. Chem. 284 (2009) 2258–2265.
[25] C.H. Chen, Platelet-activating factor acetylhydrolase: is it good or bad for you? Curr. Opin. Lipidol. 15 (2004) 337–341.
[26] M. Sheves, A. Albeck, N. Friedman, M. Ottolenghi, Controlling the pKa of the bacteriorhodopsin Schiff base by use of artificial retinal analogues, Proc. Natl. Acad. Sci. U. S. A. 83 (1986) 3262–3266.
[27] S. Pegorier, D. Stengel, H. Durand, M. Croset, E. Ninio, Oxidized phospholipid: POVPC binds to platelet-activating-factor receptor on human macrophages. Implications in atherosclerosis, Atherosclerosis 188 (2006) 433–443.
[28] T.A. Seimon, M.J. Nadolski, X. Liao, J. Magallon, M. Nguyen, N.T. Feric, M.L. Koschinsky, R. Harkewicz, J.L. Witztum, S. Tsimikas, D. Golenbock, K.J. Moore, I. Tabas, Atherogenic lipids and lipoproteins trigger CD36-TLR2-dependent apoptosis in macrophages undergoing endoplasmic reticulum stress, Cell Metab. 12 (2010) 467–482.
[29] M.E. Greenberg, X.M. Li, B.G. Gugiu, X. Gu, J. Qin, R.G. Salomon, S.L. Hazen, The lipid whisker model of the structure of oxidized cell membranes, J. Biol. Chem. 283 (2008) 2385–2396.
[30] C. Code, A.K. Mahalka, K. Bry, P.K. Kinnunen, Activation of phospholipase A2 by 1-palmitoyl-2-(9′-oxo-nonanoyl)-sn-glycero-3-phosphocholine *in vitro*, Biochim. Biophys. Acta 1798 (2010) 1593–1600.
[31] H. Esterbauer, R.J. Schaur, H. Zollner, Chemistry and biochemistry of 4-hydroxynonenal, malonaldehyde and related aldehydes, Free Radic. Biol. Med. 11 (1991) 81–128.
[32] K. Uchida, L.I. Szweda, H.Z. Chae, E.R. Stadtman, Immunochemical detection of 4-hydroxynonenal protein adducts in oxidized hepatocytes, Proc. Natl. Acad. Sci. U. S. A. 90 (1993) 8742–8746.
[33] G. Subbanagounder, N. Leitinger, D.C. Schwenke, J.W. Wong, H. Lee, C. Rizza, A.D. Watson, K.F. Faull, A.M. Fogelman, J.A. Berliner, Determinants of bioactivity of oxidized phospholipids. Specific oxidized fatty acyl groups at the sn-2 position, Arterioscler. Thromb. Vasc. Biol. 20 (2000) 2248–2254.
[34] B.G. Gugiu, K. Mouillesseaux, V. Duong, T. Herzog, A. Hekimian, L. Koroniak, T.M. Vondriska, A.D. Watson, Protein targets of oxidized phospholipids in endothelial cells, J. Lipid Res. 49 (2008) 510–520.
[35] J. Huber, A. Vales, G. Mitulovic, M. Blumer, R. Schmid, J.L. Witztum, B.R. Binder, N. Leitinger, Oxidized membrane vesicles and blebs from apoptotic cells contain biologically active oxidized phospholipids that induce monocyte-endothelial interactions, Arterioscler. Thromb. Vasc. Biol. 22 (2002) 101–107.
[36] L.C. Huber, A. Jungel, J.H. Distler, F. Moritz, R.E. Gay, B.A. Michel, D.S. Pisetsky, S. Gay, O. Distler, The role of membrane lipids in the induction of macrophage apoptosis by microparticles, Apoptosis 12 (2007) 363–374.
[37] S. Diment, M.S. Leech, P.D. Stahl, Cathepsin D is membrane-associated in macrophage endosomes, J. Biol. Chem. 263 (1988) 6901–6907.
[38] K. Kagedal, U. Johansson, K. Ollinger, The lysosomal protease cathepsin D mediates apoptosis induced by oxidative stress, FASEB J. 15 (2001) 1592–1594.
[39] K.J. Smith, W.O. Twal, F. Soodavar, G. Virella, M.F. Lopes-Virella, S.M. Hammad, Heat shock protein 70B′ (HSP70B′) expression and release in response to human oxidized low density lipoprotein immune complexes in macrophages, J. Biol. Chem. 285 (2010) 15985–15993.
[40] E. Al-Shawaf, J. Naylor, H. Taylor, K. Riches, C.J. Milligan, D. O'Regan, K.E. Porter, J. Li, D.J. Beech, Short-term stimulation of calcium-permeable transient receptor potential canonical 5-containing channels by oxidized phospholipids, Arterioscler. Thromb. Vasc. Biol. 30 (2010) 1453–1459.
[41] S. bu-Hamad, N. Arbel, D. Calo, L. Arzoine, A. Israelson, N. Keinan, R. Ben-Romano, O. Friedman, V. Shoshan-Barmatz, The VDAC1 N-terminus is essential both for apoptosis and the protective effect of anti-apoptotic proteins, J. Cell Sci. 122 (2009) 1906–1916.
[42] Y.S. Bae, J.H. Lee, S.H. Choi, S. Kim, F. Almazan, J.L. Witztum, Y.I. Miller, Macrophages generate reactive oxygen species in response to minimally oxidized low-density lipoprotein: toll-like receptor 4- and spleen tyrosine kinase-dependent activation of NADPH oxidase 2, Circ. Res. 104 (2009) 210–218 21 pp.
[43] C. Erridge, S. Kennedy, C.M. Spickett, D.J. Webb, Oxidized phospholipid inhibition of toll-like receptor (TLR) signaling is restricted to TLR2 and TLR4: roles for CD14, LPS-binding protein, and MD2 as targets for specificity of inhibition, J. Biol. Chem. 283 (2008) 24748–24759.
[44] J. Liu, S.M. Deyoung, M. Zhang, L.H. Dold, A.R. Saltiel, The stomatin/prohibitin/flotillin/HflK/C domain of flotillin-1 contains distinct sequences that direct plasma membrane localization and protein interactions in 3T3-L1 adipocytes, J. Biol. Chem. 280 (2005) 16125–16134.
[45] L. Snyers, E. Umlauf, R. Prohaska, Association of stomatin with lipid–protein complexes in the plasma membrane and the endocytic compartment, Eur. J. Cell Biol. 78 (1999) 802–812.
[46] U. Salzer, R. Prohaska, Stomatin, flotillin-1, and flotillin-2 are major integral proteins of erythrocyte lipid rafts, Blood 97 (2001) 1141–1143.
[47] M. Mairhofer, M. Steiner, W. Mosgoeller, R. Prohaska, U. Salzer, Stomatin is a major lipid-raft component of platelet alpha granules, Blood 100 (2002) 897–904.
[48] U. Reiss, B. Oskouian, J. Zhou, V. Gupta, P. Sooriyakumaran, S. Kelly, E. Wang, A.H. Merrill Jr., J.D. Saba, Sphingosine-phosphate lyase enhances stress-induced ceramide generation and apoptosis, J. Biol. Chem. 279 (2004) 1281–1290.